Biophysical Journal Volume 66 May 1994 1290–1300

Electrostatic Potentials and Electrostatic Interaction Energies of Rat Cytochrome b_5 and a Simulated Anion-Exchange Adsorbent Surface

David J. Roush, Davinder S. Gill, and Richard C. Willson*
Department of Chemical Engineering, University of Houston, Houston, Texas 77204-4792 USA

ABSTRACT Electrostatic potentials were determined for the soluble tryptic core of rat cytochrome b_5 (using a structure derived from homology modeling) and a simulated anion-exchange surface through application of the linearized finite-difference Poisson-Boltzmann equation with the simulation code UHBD. Objectives of this work included determination of the contributions of the various charged groups on the protein surface to electrostatic interactions with a simulated anion-exchange surface as a function of orientation, separation distance, and ionic strength, as well as examining the potential existence of a preferred contact orientation. Electrostatic interaction free energies for the complex of the model protein and the simulated surface were computed using the electrostatics section of UHBD employing a 110^3 grid. An initial coarse grid spacing of 2.0 Å was required to obtain correct boundary conditions. The boundary conditions of the coarse grid were used in subsequent focusing steps until the electrostatic interaction free energies were relatively independent of grid spacing (at approximately 0.5 Å). Explicit error analyses were performed to determine the effects of grid spacing and other model assumptions on the electrostatic interaction free energies. The computational results reveal the presence of a preferred interaction orientation; the interaction energy between these two entities, of opposite net charge, is repulsive over a range of orientations. The electrostatic interaction free energies appear to be the summation of multiple fractional interactions between the protein and the anion-exchange surface. The simulation results are compared with those of ion-exchange adsorption experiments with site-directed mutants of the recombinant protein. Comparisons of the results from the computational and experimental studies should lead to a better understanding of electrostatic interactions of proteins and charged surfaces.

INTRODUCTION

Theoretical understanding of electrostatic interactions involving proteins dates to the work of Tanford and Kirkwood (1957), and computational investigation has been developed further by many others as reviewed by Davis and McCammon (1990). Linearized finite difference Poisson-Boltzmann (LFPB) methods have been used extensively to compute the electrostatic energies and potentials of proteins (Gilson et al., 1985; Warwicker et al., 1985; Klapper et al., 1986; Head-Gordon and Brooks, 1987; Sharp et al., 1987; Gilson and Honig, 1987; Weber et al., 1989). Electrostatic interactions of biopolymers, including DNA and protein-DNA interactions, have been explored using the LFPB technique (Zacharias et al., 1992) and by Monte Carlo simulations (Jayaram et al., 1990, 1991). The results of Monte Carlo and Poisson-Boltzmann simulations as a function of ionic strength for the enzyme-substrate system including superoxide dismutase have been compared (Bacquet et al., 1988; Getzoff et al., 1992). The importance of including the appropriate reference state (Gilson and Honig, 1988a, b) and of accounting for errors resulting from finite difference calculations has been addressed in the literature (Gilson et al., 1987; Mohan et al., 1992). It is also computationally feasible to apply the nonlinear Poisson-Boltzmann equation to relatively small systems (Sharp and Honig, 1990). This is especially important for the simulation of species of high charge density, such as DNA (Jayaram et al., 1989).

Experimental studies have indicated that electrostatic interactions are involved in the specificity of retinol binding proteins (Jakoby et al., 1993), which involve several modes of binding. Previous work in this area involved modeling the electrostatic potentials of lipid bilayers (Zheng and Vanderkooi, 1992) and modeling the interactions of glycolipids at membrane surfaces (Ram et al., 1992). Recently, the redox properties of membrane-spanning proteins of the cytochrome b family have been modeled with limited success (Krishtalik et al., 1993), because the results are model-dependent.

This study examines the influence of relative orientation and separation distance on the electrostatic free energy of interaction of rat cytochrome b_5 and a simulated anion-exchange adsorbent surface. The existence of a preferred binding orientation is investigated and compared with experimental studies of ion-exchange adsorption of site-directed charge mutants of this protein.

Received for publication 13 October 1993 and in final form 28 January 1994.

Address correspondence to Richard C. Willson, Departments of Chemical Engineering and Biochemical and Biophysical Sciences, University of Houston, Houston, TX 77204-4792. Tel.: 713-743-4308; Fax: 713-743-4323.

D. S. Gill's present address is: Department of Surgery, Massachussetts General Hospital and Harvard Medical School, Boston, MA 02114.

0006-3495/94/05/1290/11 $2.00

METHODS

Model

The coordinates of the soluble tryptic fragment of rat cytochrome b_5 were derived from a homology model based on the crystal structure of the homologous bovine protein (Gill et al., 1993), with the solvation waters removed through editing of the PDB file. Cytochrome b_5 is well suited for use

in studies of anion-exchange adsorption because of its great stability in solution, moderate molecular weight (M_r = 13,603), and negative net charge at pH values near neutrality—pI 4.6 by isoelectric focusing (IEF), 23 negative charges (including the fractional ionization of groups in the protoporphyrin prosthetic group), and 15 positive groups (allowing for partial titration of histidines) resulting in a net charge −9.4 at pH 8.0. The information on histidine titrations was based on NMR data of Altman et al. (1989).

The ion-exchange surface functional group model is based on information provided by Pharmacia for derivatization of Mono Q, the monodisperse adsorbent used in the experimental studies. The quaternary amine group affixed to the hydrophilic substrate is -O-CH_2-N-$(CH_3)_3$. A methyl group was appended to the oxygen atom to complete the bond coordination. The structure was created in ChemNote under Quanta (version 3.2; Molecular Simulations, Inc., Waltham, MA) employing CHARMm parameters (Brooks et al., 1983; version 20.3) for the atoms. The carbons were all treated as CT, the nitrogen as NP, and the hydrogens as either HC or HA, depending on their location. The coordination of the nitrogen was defined as sp^3 hybridization in a tetrahedral geometry to be refined later through minimization and equilibration. The nitrogen was originally assigned a fixed charge of +1.0 and the molecule was imported into QUANTA (with the parameter set of reconverting all atoms without using rule based charges) with appropriate charge redistribution to meet fractional atomic charge distribution constraints, resulting in a charge of 0.93 on the nitrogen. The atomic charges and van der Waals radii for the ion-exchange surface atoms used in the electrostatics calculations were based on the data file param203.par from the CHARMm version 20.3 database. The residue functionality was treated as IONEI. The fractional charges of the ion-exchange residues used in the electrostatic calculations are as follows: NP +1.00, CT (methyl group of quaternary amine) +0.050, HC (associated with methyl group of quaternary amine) +0.02, CT (backbone C adjacent to NP and terminal methyl group) −0.02, HA (associated with terminal methyl group) 0.00, and OE (backbone O) −0.41. The parameter set for the protein molecule was based on the OPLS data set, with the exception of the parameters for the heme protoporphyrin IX, for which the data were obtained from the PORPHYRIN.RTF and the param203.par files from the CHARMm version 20.3 database.

The ion-exchange functional group (quaternary amine with spacer arm) was solvated in an 8.0 Å spherical water shell (including 189 TIP3S water molecules) for use in the ensuing MD calculations. A modification of the method of Shen et al. (1989) was employed for minimization and equilibration of the functional group and was performed as follows. The functional group was constrained while the solvation waters underwent 100 steps of Adopted Basis set Newton-Raphson (ABNR) followed by heating to 300 K over 20 ps. Once the solvation waters had reached 300 K, 20 ps of dynamic equilibration were performed with the functional group constrained. SHAKE (with a tolerance of 1×10^{-9}) was applied to the functional group in all cases henceforth. The water was then constrained while performing 100 steps of steepest descent on the functional group; the functional group reached minimum energy (within the specified default tolerance) after 35 steps. Another 100 steps of steepest descent were performed on the functional group followed by 100 steps of ABNR to ensure minimization of energy. The water was constrained, and the functional group was heated to 100 K over 10 ps followed by 5 ps of dynamic equilibration at 100 K. The structure was then heated to 200 K over 10 ps followed by 5 ps of dynamic equilibration, with the waters constrained. Finally, the structure was heated to 300 K over 10 ps, with the waters constrained, followed by 30 ps of dynamic equilibration with the waters unconstrained. The solvation waters were removed from the structure through editing of the PDB file, before continuum calculations.

Estimation of a suitable charge density and surface area for interaction were critical components in the design of the simulated surface. The charge density on the simulated surface is a parameter that can be changed easily, and information on the charge density of the experimental ion-exchange surface is not available. Hence, the surface was constructed so as to minimize the effect of nonuniform charge distribution on the surface by use of a square grid. Nine functional groups were arranged in a 3 × 3 array with the y plane of the ion-exchange surface passing perpendicularly through the N of the functional groups and with a separation distance of 18 Å to yield a reasonable charge density (approximately 10 $\mu C/cm^2$) on the surface. This arrangement of functional groups yields a total surface area slightly greater than the cross-sectional area of the protein. The dielectric constant was chosen as 4.0 for interior of the functional groups in the simulated surface based on the chemical nature of the spacer arm and the functional groups involved. A simplification of the surface exists in this planar representation because the back side of the ion-exchange surface is treated as a continuum of high dielectric, whereas the nature of the dielectric constant for true experimental surface is unknown. This simplification should not affect significantly the electrostatic interaction energies because the quaternary amine functional group is located on the front of the surface, with very few charge-bearing atoms located on the back of the ion-exchange spacer arm.

Calculations of electrostatic energies

The electrostatic free energies of interaction of the protein and the simulated anion-exchange surface were determined using the electrostatics portion of the University of Houston Brownian Dynamics code (UHBD; Davis et al., 1991) to solve the linearized Poisson-Boltzmann equation with a finite-difference algorithm. The linearized form of the PB is computationally more efficient than the nonlinearized PB (Zacharias et al., 1992) and is appropriate for the electrostatic potentials and charge densities studied in this system, as discussed below. The interiors of the protein and of the ion-exchange functional groups are treated as low dielectric regions of a fixed polarizability. The solvent is treated as a high dielectric continuum with a representation of a Boltzmann weighting of counterions and coions in regions outside the molecules.

Initial calculations were performed on a 110^3 cubic grid with the molecule(s) mapped onto the grid based on the location of the geometric center, as calculated by UHBD. The grid was centered on the geometric center of each individual species when calculated separately and on the geometric center of complex for interaction energy calculations. The methods used to conserve charge distribution, monopoles, and dipoles for irregularly shaped species when placed onto a finite-difference grid are covered elsewhere (Zacharias et al., 1992; Davis et al., 1991; Edmonds et al., 1984). The dielectric constants at the grid points corresponding to the solvent (ϵ_s) and to the protein and adsorbent interiors (ϵ_p) were assigned values of 78.0 and 4.0, respectively (Gilson and Honig, 1986). Dielectric boundary smoothing, yielding intermediate dielectric constants, was applied to grid lines that fell on the boundary between the high and low dielectric regions (Davis and McCammon, 1991). Each atom was treated as a Debye-Hückel sphere, and the potential at the boundary calculated as the analytical sum of the potentials of the individual atoms. Initial grids for both the complex and the individual species were then focused (Klapper et al., 1986; Gilson et al., 1985; Zacharias et al., 1992) to lattice sizes at which the energies converged within the computational errors.

The derivation of the methodology for finite-difference solution of the linearized Poisson-Boltzmann equation employed by UHBD has been described elsewhere (Davis and McCammon, 1989). Electrostatic interaction free energies for the complex can be calculated using the analytical form of Coulomb's equation combined with the values of the electrostatic energies computed by the finite difference calculations as previously described (Gilson and Honig, 1988a; Gilson and Honig, 1988b; Luty et al., 1992) and extended by Luty (1993), whose nomenclature is used below.

The total electrostatic free energy of a macromolecular species is equal to the summation of the Coulombic energy of assembling the solute atoms (relative to a reference state at infinite separation in a uniform medium of dielectric constant of 4.0) and the reaction field energy. To compute the electrostatic free energies of the species and the complex, one must compute the electrostatic potentials. The electrostatic potential for a finite difference grid calculation is composed of three parts

$$\phi_i = \phi_i^s + \phi_i^{C(FD)} + \phi_i^x \quad (1)$$

where ϕ_i is the electrostatic potential at charge i and ϕ_i^s corresponds to the self potential at charge i that would be created by charge i (without interactions with other charges) in an infinite medium of dielectric constant ϵ_p. $\phi_i^{C(FD)}$ is the finite difference Coulomb potential or the potential at charge i which would be caused by all other charges on the grid in an infinite

medium of dielectric constant ϵ_p, and ϕ_i^x is the reaction potential generated by the solvent and the mobile ions at charge i. These contributions must be determined for each individual species as well as the complex in order to calculate the interaction energy. The reaction field free energy for the LPB can be expressed as follows

$$\Delta G^x = \frac{1}{2}\sum_{i=1}^{N} q_i \phi_i^x \quad (2)$$

where ΔG^x is the sum over all the atomic charges q_i, multiplied by the electrostatic potential at charge i caused by the solvent and mobile ions, ϕ_i^x.

Computational memory restrictions required that boundary conditions be determined from a single large grid at coarse grid spacing, followed by focusing calculations performed on two separate smaller grids. Electrostatic free energies for each molecule were determined by performing the finite difference calculation: (1) with the molecule immersed in a medium of high dielectric ($\epsilon_s = 78$) and ionic strength of 100 mM, except as noted; (2) with the molecule immersed in a uniform low dielectric ($\epsilon_s = \epsilon_p = 4.0$); followed by (3) an analytical solution for the molecule in a uniform low dielectric ($\epsilon_s = \epsilon_p = 4.0$). The total electrostatic energy is computed by subtraction of (2) from (1) and addition of (3). Each calculation must be performed for both the individual species and the complex because different grids were used in the calculations, as discussed below. The electrostatic interaction free energy of the complex is computed by subtracting the sum of the total electrostatic energies of the two species from that of the complex. All electrostatic calculations were performed at a temperature of 300 K, with the associated ionic strength and ion distribution. Preliminary calculations employing a Silicon Graphics, Inc. 4D/320 VGX computer with 96 Mbytes memory required approximately 31 CPU hours to complete one binding energy calculation. Production runs performed using the highly vectorized version of UHBD on a Cray Y-MP 84 required approximately 1.2 SU for each binding energy calculation.

To obtain meaningful results from LFPB calculations, it is essential to establish convergence of calculated electrostatic interaction free energies, relatively independent of grid spacing, and to determine the effects of grid size on calculated interaction free energies (Mohan et al., 1992). Total electrostatic energy calculations for the individual species and for the complex indicate that a grid spacing of 0.5 Å is required to reach grid size-independent convergence of energies. The protein is roughly ellipsoidal with a major axis of 30 Å and a minor axis of 20 Å, and the simulated surface is of dimensions 40 Å × 40 Å × 10 Å (including molecular size). To allow for accurate approximation of the boundary conditions by the Debye-Hückel equation, a border of 5 to 10 Å must be allowed between the edge of the complex and the edge of the simulation grid (Zacharias et al., 1992). For a 5 Å separation distance, the minimum examined in this study, these restrictions imply a minimum total system size of approximately 55 Å × 55 Å × 55 Å. The current vectorized version of UHBD allows for a maximum grid size of 110^3, thereby restricting the size of the complex to be studied to be of maximum dimensions 45 Å × 45 Å × 45 Å, before the addition of the 5-Å border. Therefore, for most of the separation distances of interest, the complex exceeds the maximum size that can be examined directly, and the use of two grids was required for final focusing of the complex.

It is necessary to perform a calculation on the entire system at a coarse grid spacing (2 Å), where the size of the species is a small fraction of the overall grid dimensions, to obtain the appropriate boundary conditions (Gilson et al., 1988). The initial boundary conditions obtained from the coarse grid spacing are then used in a series of focusing steps to a final grid spacing of 0.5 Å. To reach this fine grid spacing, the protein must be divided into two sections due to the size of the protein/ion-exchange system. The association energy of one part of the protein with the simulated surface is then calculated based on the boundary conditions focused from the initial coarse calculation. The remainder of the protein and its association energy with the simulated surface are also focused to 0.5 Å based on boundary conditions from the coarse calculation.

To determine an estimate of the error for the interaction energy associated with dividing the protein molecule into two parts, calculations were performed for the protein molecule as a single unit and as the two separate units for each protein orientation for grid spacings ranging from 1.5 to 0.5 Å. Comparisons were made between the energies for the entire protein molecule and the summation of the energies of the two separate species at 0.5 Å grid spacings. Because previous investigators (Gilson et al., 1988b) have used rotational averaging of electrostatic energies to reduce the error associated with a particular grid placement, the effect of varying the orientation on the calculated total electrostatic energy of the protein alone was also determined. The error associated with discretizing the potentials onto a grid was assessed by performing the interaction energy calculations for the complex on a square grid of 109^3, effectively translating the entire grid one-half grid space unit from the 110^3 case and also slightly shifting the grid boundaries. To estimate the largest potential error associated with changing the grid dimensions, the electrostatic energies for the protein and the ion-exchange surface calculated individually using the 109^3 grid were subtracted from the electrostatic energies for the complex calculated using 110^3 grid for each orientation and separation distance examined.

Calculations over a range of orientation and separation distances

The coordinates and initial orientation for the protein were taken from the homology model cited above. The reference orientation for the protein with respect to the vertical (y) axis is a zero degree rotation. The ion-exchange surface is located in an orientation parallel to the y-z plane, with the functional groups extending in the x plane. The simulated ion-exchange surface was centered with respect to the protein's cross section and separated from it by approximately 10 Å. Separation distance between the protein and the simulated surface is defined throughout this work as the distance of closest approach for any functional group of the protein to the furthest extension of the simulated surface in the x direction.

Geometrical calculations were performed with UHBD to determine the geometric centers for the individual species and the complex as well as separation distances between the two species. To determine the effect of protein orientation on the electrostatic interaction energy of the complex, the protein was rotated about an axis passing through its geometric center and parallel to the y axis. The rotation about the y axis was chosen as a representative case, because rotations of the protein about the combinations of the x, y, and z axes were computationally prohibitive. The protein is asymmetrical and, therefore, the separation distance between the protein and simulated surface changes as a function of rotation of the protein about the y axis. The protein was then translated, if necessary, along the x axis to achieve the specified separation distance. The electrostatic interaction free energies for the complex of the protein and the ion-exchange surface were computed over a range of rotations about the y axis of 0 to 335° for separation distances of 5, 10, 15, and 20 Å. Interaction energies were also calculated for several intermediate separation distances for the 90° orientation, as discussed below.

RESULTS

The Cα trace of the predicted tertiary structure of the soluble tryptic core of rat cytochrome b_5 (with the protoporphyrin prosthetic group) is presented in Fig. 1 (Gill et al., 1993). A representation of the distribution of charged residues is depicted on the diagram to aid in interpretation of the interaction results. The N- and C-termini of the protein are located on the upper right and bottom-center of the image, respectively. The electrostatic interaction free energies of the model protein and the simulated surface were computed at separation distances in the range of 5 to 20 Å employing the LPB. The smallest grid spacing that would still allow for correct boundary conditions was employed for the cases where the size of the complex dictated the overall grid dimensions. Because the protein is asymmetrical, the size of the system

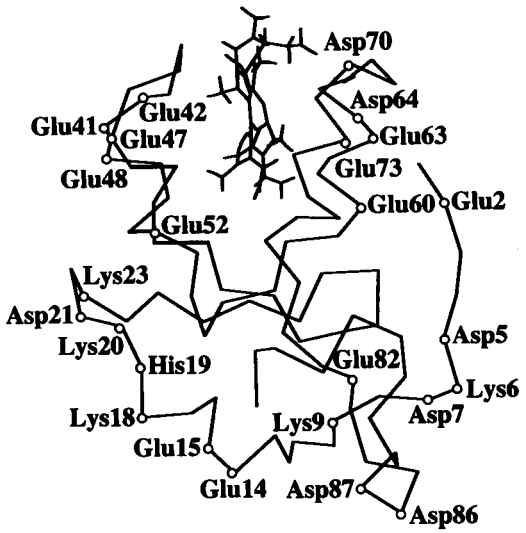

FIGURE 1 Cα trace of the proposed tertiary structure of the soluble core of rat cytochrome b_5 (with the heme prosthetic group) indicating some of the various charged functional groups on the surface of the protein.

varied as a function of orientation, leading to different smallest achievable grid spacings. The electrostatic interaction free energies were computed with grid spacings of 0.5 Å for separation distances of 5.0 and 10 Å (0.6 Å for the 335° orientation at 10 Å) but not for all of the orientations at greater separation distances. For the 15 Å separation distance, the smallest grid spacing of 0.5 Å was still achieved for most cases with the exception of 0, 45, 60, 270, and 335° *y* rotation (0.6 Å). For the 20 Å separation distance, the 0.5 Å grid spacing was used for the calculations, with the exception of 45 and 90° *y* rotation (0.6 Å) and 0, 60, 270, and 335° *y* rotation (0.8 Å).

As mentioned in Methods, convergence of the total electrostatic energies for the two species is required to obtain an accurate estimate of the interaction energy. Fig. 2 shows the convergence of interaction energy as a function of grid spacing for the 60, 135, and 270° *y* rotations at a 5 Å separation distance. It is evident from the figure that the interaction energies have not converged for grid spacings larger than 0.8 Å. The errors represented by the error bars originate from the coarse representation of the charges and electrostatic potentials at large grid spacings and arise approximately equally from grid dimension changes and from representing the protein molecule as two species.

The electrostatic interaction free energy of the complex as a function of separation distance and orientation is presented in Fig. 3. Error bars for the data points were calculated as the summation of the estimated errors associated with dividing the molecule into two parts (as described in the Model section) and those associated with the grid dimensions (the difference in the total electrostatic energies, at 0.5 Å grid spacing, of the protein mapped onto a 110^3 and onto a 109^3 grid). The analytical Coulombic energies and reaction field energies for the protein in the unbound state were calculated at each *y* rotation and employed for calculation of the electrostatic interaction free energies of the complex. The error associated with the rotation of the protein molecule about the *y* axis for all separation distances was on average 0.69 kcal/mole with a standard deviation of variation with rotation of 1.23 kcal/mole and was calculated from the difference in total electrostatic energy of the protein at a given orientation and at the 0° orientation. Generally, the error in the total electrostatic energy associated with the rotation of the protein is significantly smaller than the errors from dividing the protein molecule into two parts and from changing the grid dimensions from 110^3 to 109^3.

As illustrated in Figure 3, the interaction free energy is a strong function of orientation and shows a broad minimum between 60 and 90° *y* rotation. The protein residues closest to the ion-exchange surface at this favored interaction (90° *y* rotation at 5 Å separation distance) are Glu47, Glu48, Ser68, Asp70, Arg72, and Glu73 (surrounding the heme prosthetic group). A comparably low interaction energy exists for the 60° *y* rotation with residues Glu60, Asp64, Gly66, His67, Ser68, and Thr69 closest to the ion-exchange surface for the range of separation distances 10 to 20 Å. The interaction energy then increases and actually leads to a repulsion

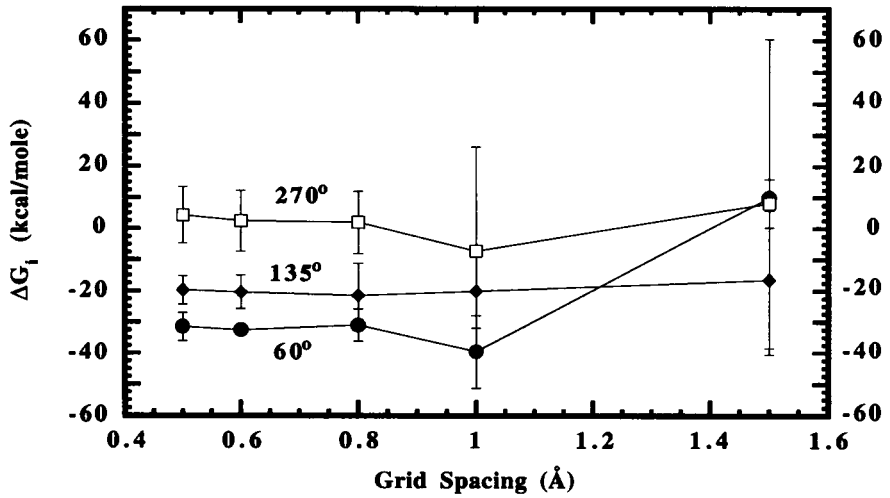

FIGURE 2 A plot of the interaction free energy of rat cytochrome b_5 with a simulated anion-exchange surface as a function of grid spacing for the *y* rotations of 60, 135, and 270° at a 5 Å separation distance. The plot illustrates the importance of grid spacing in convergence of interaction energies. The error bars represent the summation of errors resulting from grid discretization (109^3 vs. 110^3) and resulting from representing the protein molecule on one or two grids.

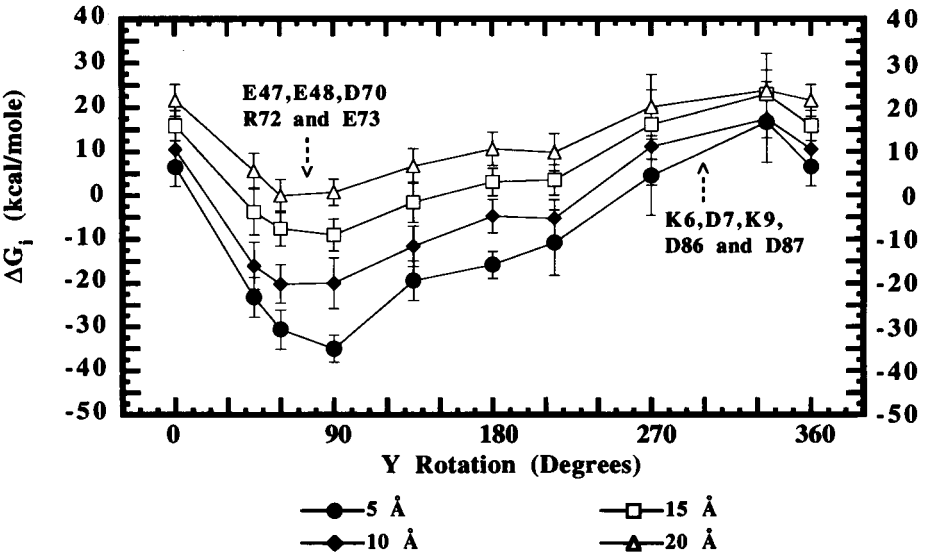

FIGURE 3 A plot of the interaction free energy of rat cytochrome b_5 and a simulated anion-exchange surface as a function of separation distance and orientation. All calculations were performed with 100 mM ionic strength, pH 8.0, and a temperature of 300 K. The interaction free energies were computed as described in Methods. Error bars are based on summation of errors associated with the computational method.

between 270 and 360° y rotation. At 270° y rotation, the residues closest to the ion-exchange surface include Lys6, Asp7, Val8, Lys9, Tyr10, His84, Pro85, Asp86, and Ser89 on the protein surface opposite to the heme prosthetic group. The maximum in the repulsive interaction occurs at 335° y rotation, and the closest residues to the ion-exchange surface are Lys6, Asp7, Pro85, Asp86, Asp87, and Ser89.

The calculations of the interaction energies were performed with the protein centered with respect to the ion-exchange surface. To determine the effect of translation of the protein parallel to the ion-exchange surface (or parallel to the y axis), a test calculation was performed for the case of 90° y rotation and 5 Å separation distance, both with and without a 5 Å y translation. The results were interaction energies of −34.37 kcal/mole (with 5 Å y translation) and −34.98 kcal/mole (without 5 Å y translation). These values differ by an amount well within the error associated with the interaction energy under these conditions (3.06 kcal/mole). The potential effects of x rotation combined with y rotation on the interaction energies were examined. Interaction energies were determined at a separation distance of 5 Å over the range of y rotations 0 to 180° and for x rotations of 45.0, 0.0, and −45.0°. The general shape of the interaction energy function over the range of y rotation (0.0 to 180.0°) was unchanged by either of the x rotations (45.0 or −45.0°). The difference in the interaction energies for the range of x rotations for each y rotation was either within or slightly larger than the error associated with the interaction energy calculation. The overall minimum in the interaction energy was still observed at the 5 Å separation distance, 90° y rotation and 0.0° x rotation.

The electrostatic equipotential surfaces for the protein and ion-exchange surface were computed separately, and the two images were merged to visualize more readily the interacting groups. A representation of electrostatic equipotential surfaces for the protein and the simulated ion-exchange surface for the protein in an orientation of negative interaction free energy (180° y rotation and 5 Å separation distance) is presented in Fig. 4. The discrete nature of the ion-exchange functional groups on the simulated surface is readily apparent in Fig. 4. A better visualization of the potential anion-exchange contact region on the protein surface can be obtained by illustrating the protein equipotential surfaces independently. Fig. 5 illustrates an end-on view of the electrostatic equipotential surfaces for the protein in the apparent preferred chromatographic contact region surrounding the protoporphyrin heme prosthetic group. Three major clusters of negative potential are visible in Fig. 5: (1) on the left center is the cluster containing Glu47, Glu48, and Glu52; (2) on the lower left is the cluster containing Glu41 and Glu42; and (3) on the lower right is the cluster containing Asp70 and Glu73. Fig. 6 illustrates the electrostatic equipotential surfaces for the protein surface on the opposite end of the protein, containing the cluster of Glu14 and Glu15 (right center). Contributions from the positively charged residues in the vicinity including Lys6, Lys9, and Lys20 lead to the overall repulsive interaction with the simulated surface in this orientation.

From Fig. 3, it is clear that the interaction energy decreases substantially (more than the error associated with the calculation) when the separation distance is increased from 5 to 10 Å (κ^{-1} is 9.61 Å in 100 mM ionic strength, 1:1 electrolyte and 25°C; Hiemenz, 1977). Interaction energies decrease, and the selectivity for the preferred interaction orientation decreases as the separation distance is increased to 20 Å. At the 20 Å separation distance, no significant interaction energy exists (where a favorable interaction energy was determined for smaller separation distances) between the protein and the simulated anion-exchange surface within the error of the calculation, 4.70 kcal/mole, with an SD of variation with rotation of 1.78 kcal/mole. A significantly positive (repulsive) interaction energy exists for the 270 to 360° orientations. The decrease in interaction energy arises naturally from the Debye-Hückel model employed (the boundary potential is taken as the summation of the contributions of each atom treated individually as a Debye-Hückel sphere), which

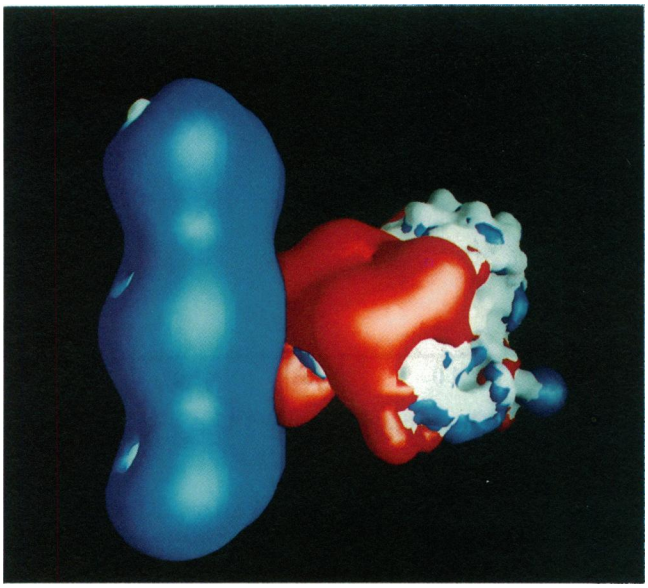

FIGURE 4 Rat cytochrome b_5 in an orientation of negative interaction free energy (180° *y* rotation and 5 Å separation distance) with the simulated anion-exchange surface. Electrostatic equipotential surfaces are displayed for the protein and ion-exchange surface according to the following color scheme. The molecular surfaces of the protein and the ion-exchange functional groups are represented as an off-white color. The equipotential surfaces are represented for the protein at electrostatic potential values of −1.2 *kT/e* (*red*) and +0.3 *kT/e* (*blue*). The equipotential surface is represented for the ion-exchanger at a value of +0.3 *kT/e* (*blue*).
Electrostatic potential grids (for images only) of 65^3 and 1.0 Å grid spacing were computed from the program UHBD and exclude the interiors of the protein and ion-exchange functional groups. Note that the electrostatic equipotential surfaces were computed individually and brought together for visualization purposes. The potential grids were converted to DelPhi electrostatic potential grids using the program Convert (M. Gilson, University of Houston). Images were created using the program GRASP, version 1.03 (Nichols and Honig) as well as the applications Showcase and Snapshot (both from Silicon Graphics, Inc., Mountain View, CA).

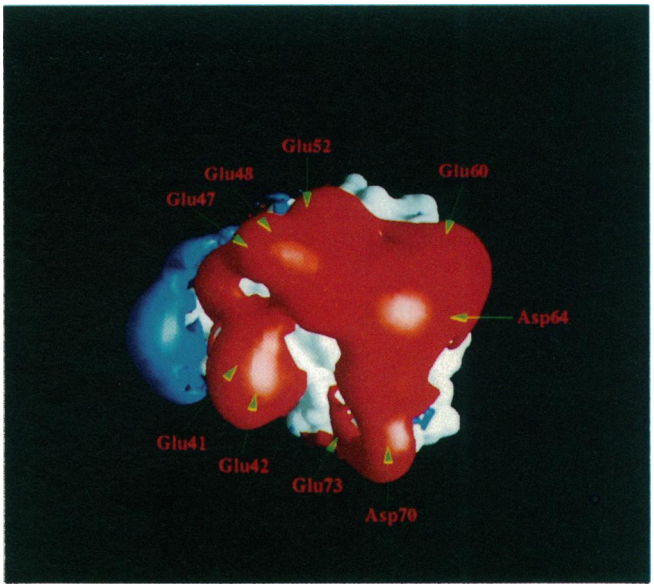

FIGURE 5 End on view of the electrostatic equipotential surfaces for the protein in the apparent preferred chromatographic contact region surrounding the protoporphyrin heme prosthetic group. This region contains the following negative clusters: a) residues Glu41, Glu 42; b) residues Glu47, Glu48, and Glu52; and c) residues Glu60 and Asp64. Other negative residues presented are Asp70 and Glu73. The equipotential surfaces are represented at electrostatic potential values of −1.2 *kT/e* (*red*) and +0.3 *kT/e* (*blue*).

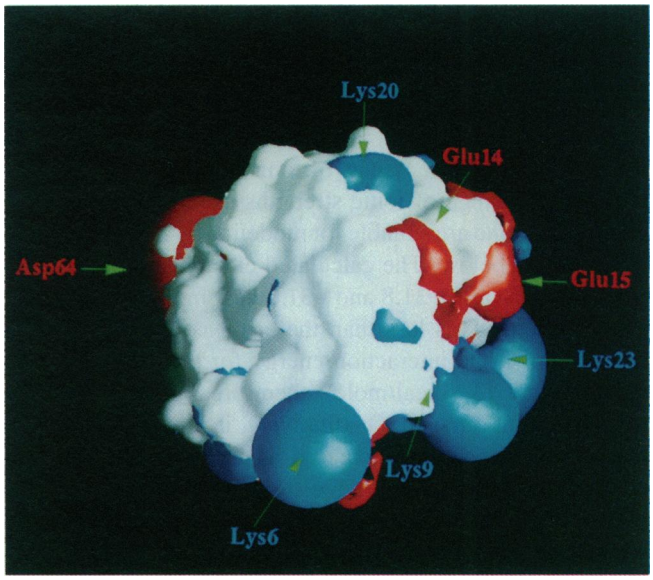

FIGURE 6 End on view of the electrostatic equipotential surfaces of the protein surface distal to the heme prosthetic group, including the residues Glu14, Glu15 and Asp64. A repulsive interaction occurs when this part of the protein is juxtaposed to the simulated anion-exchange surface. Several areas of positive charge are visible including the residues Lys6, Lys9, Lys20, and Lys23. The equipotential surfaces are represented at electrostatic potential values of −1.2 *kT/e* (*red*) and +0.1 *kT/e* (*blue*).

would predict a decrease of the electrostatic potential of a plane of charge in 100 mM ionic strength to less than 10% of the surface potential for a separation distance of 20 Å, in the absence of interactions with another double layer (Hiemenz, 1977, pp. 368–391). Hence, the influence of the charged surface on the protein would be weak at separation distances of this magnitude.

The interaction energy as a function of separation distance calculated for the most favorable orientation (90° *y* rotation) is presented in Fig. 7. As one can see from Fig. 7, the simulated anion-exchange surface appears to exhibit an electrostatic influence to approximately 17.5 Å, but no discernable influence can be seen at a separation distance of 20 Å (within the error of the calculations). A linear least-squares fit of the interaction energy versus the separation distance appears to correlate the data well, for the limited separation distance range of 5 to 20 Å. However, the correlation for these two variables may be significantly nonlinear outside of this range.

As discussed above, accurate assessment of the computational error is critical to understanding the results of the modeling. The error (error ± SD of variation with rotation) associated with dividing the protein molecule into two parts over the range of orientations studied is 3.76 ± 1.24 kcal/mole. It is less than 3.92 kcal/mole for all cases, with the

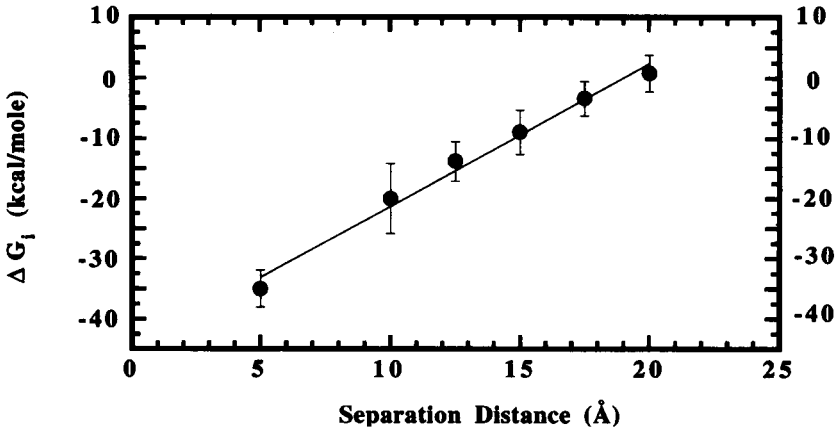

FIGURE 7 ΔG_i (kcal/mole) versus distance of closest approach for the preferred interaction orientation of 90° y rotation. All calculations were performed at 100 mM ionic strength, pH 8.0, and a temperature of 300 K. The plot illustrates the lack of interaction energy for separation distances in excess of 17.5 Å. A linear least-squares fit of the data yields the following equation

$$y = -45.0 + 2.37x : R = 0.994.$$

exception of the 270° y rotation case, where the error is 6.82 kcal/mole. The error associated with changing the grid dimensions from 110^3 to 109^3 for the 5 Å separation distance was 1.77 ± 1.76 kcal/mole. This error was less than 1.54 kcal/mole for all cases except the 215 and 335° y rotation cases, where the errors were 4.00 and 5.23 kcal/mole, respectively. As is apparent from the data, the error associated with dividing the protein molecule into two parts leads to the largest error and is the limiting factor in the accurate determination of the electrostatic interaction free energies for this large system. This error, however, is reliably smaller than the interaction energy differences among orientations and separation distances.

The influence of ionic strength on the interaction energy was investigated for the preferred interaction orientation, 90° y rotation, at a 5 Å separation distance for 75 and 125 mM ionic strength. These values of ionic strength are representative of the range of ionic strengths used in ion-exchange experiments and are suitable for modeling by LFPB analyses, as discussed below. The calculated electrostatic interaction free energies were −31.8 and −31.0 kcal/mole, respectively. The difference was less than the error associated with the calculation of the interaction energy for the 100 mM ionic strength case (3.1 kcal/mole); therefore, further investigations were not pursued. Qualitatively, it is encouraging that the interaction energy increased as the ionic strength decreased, in agreement with electrostatic screening arguments. However, for quantitative estimation of the ionic strength dependence of electrostatic interaction free energies, a Monte Carlo approach that includes ion-ion interactions may be more appropriate (Zacharias et al., 1992).

DISCUSSION

The goals of this research were to determine the effects of separation distance and orientation on the electrostatic interaction free energy of a model protein and simulated anion-exchange surface at a fixed ionic strength of 100 mM. Lower ionic strengths can be explored using the nonlinearized FPB, but as mentioned previously, for systems of this size the computations are prohibitively expensive. Previous investigators had noted an interaction energy dependence on orientation for a simplified system of lysozyme and a charged surface employing a boundary element method for solution of the linearized Poisson-Boltzmann equation (Yoon and Lenhoff, 1990; Roth et al., 1992). In this investigation, we attempt to determine the contributions of many ionizable groups over distance scales that require explicit representation of the molecular details of both the protein and ion-exchange surfaces. The feasibility of obtaining detailed atomic information from a continuum calculation has been established for the determination of pKa values of ionizable groups in proteins and other electrostatic interactions by previous investigators (Gilson and Honig, 1988; Bashford and Karplus, 1990; Zacharias et al., 1992; Gilson, 1993).

The interaction of two macromolecules involves many types of interactions, including van der Waals and hydrophobic in addition to electrostatic (examined in this investigation). Nonelectrostatic contributions to binding are not included in this computational study but could play a significant role in the actual binding of a protein to an ion-exchange surface. In contrast to the present work, Roth et al. (1992) have sought to incorporate van der Waals interactions in interaction energy calculations based on experimental surface force measurements (Pashley et al., 1985) and the inclusion of a Hamaker constant. Results from such calculations must presently be viewed with caution due to the large uncertainty in the experimentally derived parameters and the possibility that multiple types of interactions are occurring simultaneously. Although experimental data are currently limited, inclusion of all relevant types of interactions will be essential for the eventual, complete simulation of protein-surface interactions.

Another simplification used in this study was the application of the linear finite difference solution of the Poisson-Boltzmann equation. This methodology is useful when the electrostatic potential is less than k_BT and is often employed due to computational restrictions, as opposed to a full Monte Carlo treatment, especially for systems of several thousand atoms. Application of the nonlinear PB to a system of this size (1228 atoms) is computationally prohibitive. A comparison between continuum LFPB calculations and a full Monte Carlo simulation for the λ repressor-operon interaction shows a good agreement between the two methods under

many conditions (Zacharias et al., 1992). Because the continuum approach does not allow for ion-ion interactions, it provides an incomplete description of solvent-protein interactions, possibly resulting in differences observed between the two methods. Comparisons of linear and nonlinear methods, including Monte Carlo simulations with explicit ions, for the superoxide dismutase case, have been performed (Bacquet et al., 1988) and indicate a discrepancy between the calculated potentials at high ionic strengths (0.50 M) where ion-ion correlations (excluded from LFPB calculations) are significant, but good agreement between the two methods at low ionic strengths (0.10 M). For the ionic strength range examined in this study (75 to 125 mM) application of the linear PB is acceptable.

Another source of uncertainty in determining interaction energies and electrostatic potentials is the dielectric model employed. The dependence of calculated electrostatic interaction free energies on the form of the dielectric model has been examined for the packing of α-helices in globular proteins (Rogers and Sternberg, 1984) and for other biological systems, including enzyme catalysis and electron transfer (Warshel and Åqvist, 1989). For the three models examined by Rogers and Sternberg (uniform dielectric, distance-dependent dielectric, and cavity dielectric), the cavity dielectric model yielded the best results. For calculation of the rates of enzymatic catalysis, the use of microscopic dielectric constants (protein dipoles Langevin dipoles model) yielded the best results. As discussed in the Model section, the present study employed an improved method based on the cavity dielectric model, which has been established previously to successfully represent macromolecular electrostatic interaction free energies (Davis and McCammon, 1990).

A potential source of uncertainty in the interaction energy calculations is the dynamic nature of the protein structure. The structure employed for the protein was that of the average obtained from 40 ps of limited molecular dynamics simulations and was treated as static during the interaction energy calculations (see Fig. 1). The r.m.s. deviation for the Cα backbone in the core region between the 93% sequence homologous bovine x-ray structure (used as a template for the homology modeling) and the model protein is 1.28 Å, indicating a robust model. Alteration of the pKa values of the residues on the protein surface could also affect the results. For the model system explored in this study, it was assumed that the titration of the functional groups remained constant during approach to the anion-exchange surface. Other investigators have examined the effects of structural mobility on electrostatic interactions by examining the changing electrostatic potentials using computer graphical visualizations (Fisher et al., 1990). Computational restrictions limit detailed electrostatic analyses to static structures.

The contributions of the various charged residues can be investigated through the examination of site-directed mutants, both computationally and experimentally, although the potential effects of mutations on the protein tertiary structure can lead to another source of uncertainty. Previous investigators have examined the effects of mutations on the local electrostatic environment (Sharp et al., 1987; Sternberg et al., 1987; Weber et al., 1989; Getzoff et al., 1992). Computational modeling of the effects of mutations on interaction energies has been successful for several cases where a large amount of experimental data (NMR and x-ray crystallographic) on the effects of mutations is available. As recently discussed by Shi et al. (1993), the free energy change predicted to result from a charge mutation in subtilisin is model-dependent, and limitations to computational modeling of charge mutations still exist. Limited NMR (^{1}H NOESY and chemical shift) data have been acquired for several mutant forms (Glu47Gln, Glu48Gln, Glu52Gln, and Asp64Asn) of the model protein used in this study (Rodgers et al., 1988). These results revealed no significant variation in the tertiary structure as a result of the mutation, within the limitations of the data. Small conformational rearrangements on the protein surface resulting from charge mutations, however, could lead to significant changes in biological activity, as recently observed for an interleukin-1β mutant (Camacho et al., 1993), and potentially in interaction energies. The modest sensitivity of total electrostatic energies to separation distances under the conditions studied here suggests that the conclusions reached from the computational modeling would not be altered qualitatively by any but the most pronounced structural changes induced by mutation.

A further barrier to modeling of charge mutations is the potentially confounding effect of changes in the local electrostatic environment produced by charge mutations and charge reversals, including local (<4 Å) dipole effects (Warshel, 1987). Although these limitations lead to caution in interpreting results of modeling charge mutations, significant work on the understanding of these phenomena has been provided by other investigators (Russell and Fersht, 1987; Sternberg et al., 1987; Van Belle et al., 1987; Gilson and Honig, 1988a; Gilson, 1993).

The static calculations yield only the energy as a function of separation and orientation. A more dynamic model of the diffusional encounter between the protein and the ion-exchange surface, including approach and reorientation, could be obtained, although with a simplified electrostatic model of the protein. A complimentary approach has been applied by other investigators (Sines et al., 1990; Kozack and Subramaniam, 1993) which involves mutating charges on the surface of a protein and determining the relative effect on the reaction rate constant of encounter as determined through Brownian dynamics (BD) simulations including the development of an enzyme with enhanced reaction rate (Getzoff et al., 1992). Typically, a simplified version of the electrostatics is employed in these simulations to facilitate the computational efficiency. Also, at the separation distances studied in most BD simulations, the representation of the protein surface at the functional group level is not necessary (Head-Gordon and Brooks, 1987). Detailed molecular electrostatics is required, however, for determination of binding orientations in protein-protein complexes (Karshikov et al., 1992; Zhou, 1992) and for computer-aided drug design (Lybrand and McCammon, 1988; Meng et al., 1992; Ripoll et al., 1993;

Tan et al., 1993). Although simplified electrostatic interactions are common in automated docking routines involving scoring functions, they have met so far with limited success.

In preliminary computations, the relative effects of errors associated with rotation and grid dimensions were evaluated. It was determined that, for this system, the limiting error in the calculation was associated with treating the protein molecule as two separate parts. The errors associated with changing the grid dimensions and with rotational averaging were relatively small in comparison. It is worthy of note that the estimated error associated with the division of the protein could be alleviated with improved computational abilities. To reach convergence of electrostatic energies (0.5 Å grid spacing) for this model system, a grid of dimensions 140^3 is required for a separation distance of 20 Å requiring a large amount of memory, which is currently available on very few computers.

The convergence of interaction free energies that are independent of grid size, as illustrated in Fig. 2, is essential. As noted by Mohan et al. (1992), the errors arising from large grid spacings can preclude quantitative evaluation of the effects of the different variables examined. Therefore, interpretation of results for systems of this size computed from grid spacings larger than 0.8 Å should be viewed with caution.

Comparison of the simulation results with experimental results provides further insight into the electrostatic mechanisms of ion-exchange adsorption. This study investigated the contributions of various charged functional groups by examining the dependence of the interaction energy on orientation. This methodology allows for the inclusion of the long-range propagation of electrostatic potentials, through the low dielectric environment of the protein, generated by charged residues on the far side of the protein with respect to the ion-exchange surface. The continuous nature of the interaction energy profile as a function of orientation indicates that multiple surface-charged residues on the protein surface are involved in fractional electrostatic interactions with a specific functional group on the charged anion-exchange surface. This result is in agreement with experimental isocratic, isothermal HPLC chromatographic results, which indicate that neutralization of two negative charges (Glu48 and Glu52) by site-directed mutagenesis, both independently and as a double mutation, produces changes in retention behavior that are less than linearly additive in ion-exchange retention behavior. The experimental results suggest, therefore, that multiple charges could be simultaneously interacting with a single functional group on the ion-exchange surface in accord with estimates of the charge density on the experimental anion-exchange surface. The orientation-selective influence of the anion-exchange surface also appears to diminish as the separation distance increases, owing to reduced influence of particular functional groups. The agreement between the model and the experimental data increases confidence in the model.

The same preferred contact region is evident in both experimental and simulation results. The results of Fig. 3 clearly illustrate that the interaction energy is a function of orientation and that an energetic minimum occurs at a 90° y rotation. These results indicate that a preferred interaction occurs between the protein residues Glu47, Glu48, Asp70, Arg72, and Glu73 (surrounding the heme prosthetic group) and the anion-exchange surface. In this range of y rotation, the residues involved in the apparent preferred chromatographic contact region experimentally identified in both equilibrium batch adsorption (Gill et al., 1994b) and isocratic HPLC experiments are closest to the simulated anion-exchange surface. The extended minimum in the interaction energy includes a 60° y rotation and involves residues Glu60, Asp64, and His67. The residues involved in the secondary minimum correspond to a patch of residues experimentally determined to be significantly involved in anion-exchange adsorption, although to a lesser degree than those of the Glu47 patch.

It is worthy of note that no statistically significant effect on adsorption or retention behavior, compared to the wild type protein, was found for the site-directed charge mutant Glu15Gln on the side of the protein opposite the preferred contact region from both the equilibrium batch adsorption (Gill et al., 1994b) and the isocratic HPLC experiments. The calculated repulsive interaction energy at orientations juxtaposing this residue suggests that this residue is probably not involved in the anion-exchange adsorption for this protein. Therefore, removing this negative charge by site-directed mutagenesis does not affect the observed adsorption behavior of the protein. The slight decrease in repulsive interaction energy that occurs at 0° (360°) rotation (as compared with the 335° rotation) probably results from the inclusion of Asp64 in the interaction with the simulated surface.

The distance dependence of the electrostatic interaction free energy of the protein and the simulated surface was examined over a range of separation distances (5 to 20 Å) to examine the predicted influence of long range electrostatic interactions as predicted by the linearized Poisson-Boltzmann equation. Previous investigators (Kozack and Subramaniam, 1993; Zacharias et al., 1992) have estimated the extent of influence of charged functional groups in a continuum solvent environment (greater than standard deviations of the errors associated with the calculations) to be up to 18 and 25 Å, respectively, when finite difference methods were used to compute the reaction rate constants for the Brownian dynamics encounter of the antibody HYHEL-5 (at 150 mM ionic strength) and lysozyme, and the interaction of the λ repressor-operon complex (at 22 mM ionic strength).

The effects of electrostatic forces on the protein as it approaches the ion-exchange surface are interesting to consider because the protein can experience either a strongly attractive or repulsive interaction free energy over the range of orientations. From Fig. 3, it is possible that a protein molecule placed in a 180° orientation would rotate to reach an energetic minimum at a 90° rotation. The question as to whether the protein placed in a repulsive orientation, 270° rotation, would rotate as a result of the electrostatic forces from the ion-exchange surface or would diffuse away from the surface

as a result of the repulsive interaction energy can only be addressed through calculation of the electrostatic forces. It has been demonstrated that the electrostatic forces can be calculated from the grid-calculated potentials (Davis and McCammon, 1990) for small systems, but computational limitations currently restrict its use only to small molecules.

CONCLUSIONS

This study demonstrates that a modified LFPB method can be used to calculate electrostatic interaction energies for large systems (up to 1230 atoms) while still retaining information on individual atomic contributions. The computational methodology can be applied to other electrostatic interactions, including those in enzyme-receptor and protein-membrane systems. Although the influence of specific residues can be determined experimentally by site-directed mutagenesis, it is not possible to model accurately and computationally the effects of charge mutation for a generalized system. This limitation was partially overcome by geometrically examining the protein structure in the various orientations with respect to the anion-exchange surface. By examining the contributing residues over a range of orientations, the contributions of individual residues to the interaction can be estimated.

Explicit error analyses were performed to determine the relative effects of rotational averaging, changing grid dimensions, and boundaries as well as dividing a molecule into two species to the overall error associated with interaction energy calculations. It was determined that the limiting error in the calculation was the result of dividing one molecule into two species, which was required to achieve grid spacing independent convergence of electrostatic energies. The errors associated with changing the grid dimensions (from 110^3 to 109^3) and rotational averaging were relatively small by comparison. The errors in interaction energy calculations for this system were less than the effects of changes in orientation and separation distance. The results of these error analyses, in agreement with previous investigators, clearly indicate that care must be taken when interpreting results from electrostatic calculations performed with coarse grid spacings.

Hence, it is clear that the molecular electrostatics method for determining interaction free energies described is an efficient one in terms of computational requirements for large systems studied at close separation distances. The results of the simulations, in terms of interaction energy as a function of orientation, demonstrate the presence of a preferred electrostatic interaction orientation, which is in qualitative agreement with experiment.

Our appreciation is extended to Drs. Stephen Sligar, Karla Rodgers, Scott Mathews, and Tom Pochapsky for helpful discussions on the cytochrome b_5 system. We would like to thank Drs. Brock Luty (currently at DuPont-Merck), Jim Briggs, Malcolm Davis (currently at Bristol-Myers Squibb), Mike Gilson, Martin Zacharias (currently at the University of Colorado-Denver), Régis Pomes (currently at Université de Montréal), Shankar Subramaniam (currently at NCSA), and Mike Holder of the University of Houston Institute for Molecular Design for helpful suggestions on the homology and computational modeling. The work would not have been possible without access to computing resources generously provided by the Institute for Molecular Design (IMD) led by Dr. J. A. McCammon at the University of Houston. This work was supported by the Welch Foundation and by the National Science Foundation under CTS-8910087 and a Presidential Young Investigator Award to R. C. Willson. We would also like to thank the National Center for Supercomputing Applications (NCSA), University of Illinois at Urbana-Champaign, for use of the Cray Y-MP for some of the UHBD production runs.

REFERENCES

Altman, A., J. Lipka, I. Kuntz, and L. Waskell. 1989. Identification by proton nuclear magnetic resonance of the histidines in cytochrome b_5 modified by diethyl pyrocarbonate. *Biochemistry.* 28:7516–7523.

Bacquet, R. J., J. A. McCammon, and S. A. Allison. 1988. Ionic strength dependence of enzyme-substrate interactions. Monte Carlo and Poisson-Boltzmann results for superoxide dismutase. *J. Phys. Chem.* 92: 7134–7141.

Bashford, D., and M. Karplus. 1990. pKa's of ionizable groups in proteins: atomic detail from a continuum electrostatic model. *Biochemistry.* 29: 10219–10225.

Brooks, B. R., R. E. Bruccoleri, B. D. Olafson, D. J. States, S. Swaminathan, and M. Karplus. 1983. CHARMM: a program for macromolecular energy, minimization and dynamics calculations. *J. Comp. Chem.* 4: 187–217.

Camacho, N. P., D. R. Smith, A. Goldman, B. Scheinder, D. Green, P. R. Young, and H. M. Berman. 1993. Structure of an interleukin-1β mutant with reduced bioactivity shows multiple subtle changes in conformation that affect protein-protein recognition. *Biochemistry.* 32:8749–8757.

Davis, M. E., and J. A. McCammon. 1989. Solving the finite difference linearized Poisson-Boltzmann equation: a comparison of relaxation and conjugate gradient methods. *J. Comp. Chem.* 10:386–391.

Davis, M. E., and J. A. McCammon. 1990. Electrostatics in biomolecular structure and dynamics. *Chem. Rev.* 90:509–521.

Davis, M. E., J. D. Madura, B. A. Luty, and J. A. McCammon. 1991. Electrostatics and diffusion of molecules in solution: simulations with the University of Houston Brownian dynamics program. *Comp. Phys. Comm.* 62:187–197.

Davis, M. E., and J. A. McCammon. 1991. Dielectric boundary smoothing in finite difference solutions of the Poisson equation: An approach to improve accuracy and convergence. *J. Comp. Chem.* 12:909–912.

Edmonds, D. T., N. K. Rogers, and M. J. E. Sternberg. 1984. Regular representation of irregular charge distributions. Application to the electrostatic potentials of globular proteins. *Mol. Phys.* 52:1487–1494.

Fisher, C. L., J. A. Tainer, M. E. Pique, and E. Getzoff. 1990. Visualization of molecular flexibility and its effects on electrostatic recognition. *J. Mol. Graphics.* 8:125–132.

Getzoff, E. D., D. E. Cabelli, C. L. Fisher, H. E. Parge, M. S. Viezzoli, L. Banci, and R. A. Hallewell. 1992. Faster superoxide dismutase mutants designed by enhancing electrostatic guidance. *Nature.* 358: 347–351.

Gill, D. S., D. J. Roush, and R. C. Willson. 1994a. Tertiary structure of the heme-binding domain of rat cytochrome b_5 based on homology modeling. *J. Biomol. Struct. Dyn.* In press.

Gill, D. S., D. J. Roush, and R. C. Willson. 1994b. Presence of a preferred anion exchange binding site on cytochrome b_5: structural and thermodynamic considerations. *J. Chromat.* In press.

Gilson, M. K., A. Rashin, R. Fine, and B. Honig. 1985. On the calculation of electrostatic interactions in proteins. *J. Mol. Biol.* 183:503–516.

Gilson, M. K., and B. Honig. 1986. The dielectric constant of a folded protein. *Biopolymers.* 25:2097–2119.

Gilson, M., and B. Honig. 1987. Calculation of electrostatic potentials in the enzyme active site. *Nature.* 330:84–86.

Gilson, M. K., and B. Honig. 1988. Energetics of charge-charge interactions in proteins. *Proteins Struct. Funct. Genet.* 3:32–52.

Gilson, M. K., and B. Honig. 1988. Calculation of the total electrostatic energy of a macromolecular system: solvation energies, binding energies and conformational analysis. *Proteins Struct. Funct. Genet.* 4:7–18.

Gilson, M. K., K. A. Sharp, and B. Honig. 1988. Calculating the electrostatic potential of molecules in solution: method and error assessment. *J. Comp. Chem.* 9:327–335.

Gilson, M. K. 1993. Multiple-site titration and molecular modeling: two rapid methods for computing energies and forces for ionizable groups in proteins. *Proteins Struct. Funct. Genet.* 15:266–282.

Hiemenz, P. C. 1977. Principles of Colloid and Surface Chemistry. Marcel Dekker, New York. 368–391.

Head-Gordon, T., and C. L. Brooks. 1987. The role of electrostatics in the binding of small ligands to enzymes. *J. Phys. Chem.* 91:3342–3349.

Jakoby, M. G., K. R. Miller, J. T. Toner, A. Bauman, L. Cheng, E. Li, and D. P. Cistola. 1993. Ligand-protein electrostatic interactions govern the specificity of Retinol- and fatty acid-binding proteins. *Biochemistry.* 32: 872–878.

Jayaram, B., K. A. Sharp, and B. Honig. 1989. The electrostatic potential of B-DNA. *Biopolymers.* 28:975–993.

Jayaram, B., S. Swaninathan, D. L. Beveridge, K. Sharp, and B. Honig. 1990. Monte Carlo simulations on the structure of the counterion atmosphere of B-DNA. Variations on the primitive dielectric model. *Macromolecules.* 23:3156–3165.

Jayaram, B., F. M. DiCupua, and D. L. Beveridge. 1991. A theoretical study of polyelectrolyte effects in protein-DNA interactions: Monte Carlo free energy simulations on the ion atmosphere contribution to the thermodynamics of λ repressor-operon complex formation. *J. Am. Chem. Soc.* 113:5211–5215.

Karshikov, A., W. Bode, A. Tulinsky, and S. R. Stone. 1992. Electrostatic interactions in the association of proteins: an analysis of the thrombin-hirudin complex. *Protein Science.* 1:727–735.

Klapper, I., R. Hagstrom, R. Fine, K. A. Sharp, and B. Honig. 1986. Focussing of electric fields in the active site of Cu-Zn superoxide dismutase: effects of ionic strength and amino acid modification. *Proteins Struct. Funct. Genet.* 1:47–59.

Kozack, R. E., and S. Subramaniam. 1993. Brownian dynamics simulations of molecular recognition on an antibody-antigen system. *Protein Science.* 2:915–926.

Krishtalik, L. I., G.-S. Tae, D. A. Cherepanov, and W. A. Cramer. 1993. The redox properties of cytochromes b imposed by the membrane electrostatic environment. *Biophys. J.* 65:184–195.

Luty, B. A., M. E. Davis, and J. A. McCammon. 1992. Electrostatic energy calculations by a finite difference method: rapid calculation of charge-solvent interaction energies. *J. Comp. Chem.* 13:768–771.

Luty, B. A. 1993. Energetics and dynamics of biomolecules using a continuum solvent model. Dissertation, University of Houston, Department of Chemistry.

Lybrand, T. P., and J. A. McCammon. 1988. Computer simulation of the binding of an antiviral agent to a sensitive and resistant human rhinovirus. *J. Comp.-Aided Mol. Des.* 2:259–266.

Meng, E. C., B. K. Shoichet, and I. D. Kuntz. 1992. Automated docking with grid based energy evaluation. *J. Comp. Chem.* 13:505–524.

Mohan, V., M. E. Davis, J. A. McCammon, and B. M. Pettitt. 1992. Continuum model calculations of solvation free energies: accurate evaluation of electrostatic contributions. *J. Phys. Chem.* 96:6428–6431.

Nicholls, A., and B. Honig. GRASP: Graphical Representation and Analysis of Surface Properties. Columbia University, New York.

Pashley, R. M., P. M. McGuiggan, B. W. Ninham, and D. F. Evans. 1985. Attractive forces between uncharged hydrophobic surfaces: direct measurement in aqueous solution. *Science.* 229:1088–1089.

Ram, P., E. Kim, D. S. Thomson, K. P. Howard, and J. H. Prestegard. 1992. Computer modelling of glycolipids at membrane surfaces. *Biophys. J.* 63:1530–1535.

Ripoll, D. R., C. H. Faerman, P. H. Axelsen, I. Silman, and J. L. Sussman. 1993. An electrostatic mechanism for substrate guidance down the aromatic gorge of acetylcholinesterase. *Proc. Natl. Acad. Sci. USA.* 90: 5128–5132.

Rodgers, K. K., T. C. Pochapsky, and S. G. Sligar. 1988. Probing the mechanisms of macromolecular recognition: the cytochrome b_5-cytochrome c complex. *Science.* 240:1657–1659.

Roth, C. M., P. Wu, and A. M. Lenhoff. 1992. On the use of molecular structure to predict chromatographic retention. *Proceedings of AIChE 1992 National Meeting, First Topical Conference on Separations Technologies.* 526–531.

Russell, A. J., and A. R. Fersht. 1987. Rational modification of enzyme catalysis by engineering surface charge. *Nature.* 328:496–500.

Sharp, K. A., R. Fine, and B. Honig. 1987. Computer simulations of the diffusion of a substrate to an active site of an enzyme. *Science.* 236: 1458–1463.

Sharp, K. A., and B. Honig. 1990. Calculating total electrostatic energies with the nonlinear Poisson-Boltzmann equation. *J. Phys. Chem.* 94: 7684–7492.

Shen, J., S. Subramaniam, C. F. Wong, and J. A. McCammon. 1989. Superoxide dismutase: fluctuations in the structure and solvation of the active site channel studied by molecular dynamics simulation. *Biopolymers.* 28:2085–2096.

Shi, Y.-Y., A. E. Mark, C.-X. Wang, F. Huang, H. J. C. Berendsen, and W. F. van Gunsteren. 1993. Can the stability of protein mutants be predicted by free energy calculations? *Prot. Engin.* 6:289–295.

Sines, J. J., S. A. Allison, and J. A. McCammon. 1990. Point charge distributions and electrostatic steering in enzyme/substrate encounter: Brownian dynamics of modified Copper/Zinc superoxide dismutases. *Biochemistry.* 29:9403–9412.

Sternberg, M. J. E., F. R. F. Hayes, A. J. Russell, P. G. Thomas, and A. R. Fersht. 1987. Prediction of electrostatic effects of engineering of protein charges. *Nature.* 330:86–88.

Tan, R. C., T. N. Truong, and J. A. McCammon. 1993. Acetylcholinesterase: electrostatic steering increases the rate of ligand binding. *Biochemistry.* 32:401–403.

Tanford, C., and J. G. Kirkwood. 1957. Theory of protein titration curves. I. General equations for impenetrable spheres. *J. Am. Chem. Soc.* 79: 5333–5339.

Van Belle, D., I. Couplet, M. Prevost, and S. J. Wodak. 1987. Calculation of electrostatic properties in proteins: analysis of contributions from induced protein dipoles. *J. Mol. Biol.* 198:721–735.

Warshel, A. 1987. What about protein polarity? *Nature.* 330:15–16.

Warshel, A., and J. Åqvist. 1989. Electrostatic correlation of structure and function in proteins. *Chemica Scripta.* 29A:75–83.

Warwicker, J., D. Ollis, F. M. Richards, and T. A. Steitz. 1985. Electrostatic field of the large fragment of *Escherichia coli* DNA Polymerase I. *J. Mol. Biol.* 186:645–649.

Weber, P. C., T. J. Lukas, T. A. Craig, E. Wilson, M. M. King, A. P. Kwiatkowski, and D. M. Watterson. 1989. Computational and site specific mutagenesis analyses of the asymmetric charge distribution on calmodulin. *Proteins Struct. Funct. Genet.* 6:70–85.

Yoon, B. J., and A. M. Lenhoff. 1990. A boundary element method for molecular electrostatics with electrolyte effects. *J. Comp. Chem.* 11:1080–1086.

Zacharias, M., B. A. Luty, M. E. Davis, and J. A. McCammon. 1992. Poisson-Boltzmann analysis of the λ repressor-operon interaction. *Biophys. J.* 63:1280–1285.

Zheng, C., and G. Vanderkooi. 1992. Molecular origin of the internal dipole potential in lipid bilayers: calculation of the electrostatic potential. *Biophys. J.* 63:935–941.

Zhou, H.-X. 1992. Brownian dynamics study of the influences of electrostatic interaction and diffusion on protein-protein association kinetics. *Biophys. J.* 64:1711–1726.